Organic Electronics 15 (2014) 478–483

Contents lists available at ScienceDirect

Organic Electronics

journal homepage: www.elsevier.com/locate/orgel

Improved efficiency of indium-tin-oxide-free flexible organic light-emitting devices

Yue-Feng Liu [a], Jing Feng [a,*], Yi-Fan Zhang [a], Hai-Feng Cui [a], Da Yin [a], Yan-Gang Bi [a], Jun-Feng Song [a], Qi-Dai Chen [a], Hong-Bo Sun [a,b,*]

[a] State Key Laboratory on Integrated Optoelectronics, College of Electronic Science and Engineering, Jilin University, 2699 Qianjin Street, Changchun 130012, People's Republic of China
[b] College of Physics, Jilin University, 119 Jiefang Road, Changchun 130023, People's Republic of China

ARTICLE INFO

Article history:
Received 21 October 2013
Received in revised form 16 November 2013
Accepted 20 November 2013
Available online 7 December 2013

Keywords:
Organic light-emitting devices
Flexible
Ultrasmooth PEDOT: PSS anode
Template stripping

ABSTRACT

An indium-tin-oxide (ITO)-free flexible organic light-emitting device (OLED) with improved efficiency has been demonstrated by employing a template stripping process to create an ultrasmooth PEDOT: PSS anode on a photopolymer substrate. The device performance has been improved owing to lowered surface roughness of the PEDOT: PSS anode. A 38% enhancement in efficiency has been obtained. The ITO-free OLEDs on the polymer substrate have shown flexibility, and the device is free of cracks and dark spots under small bending radius. Moreover, the elimination of the H_2SO_4 residues on the surface of the H_2SO_4-treated PEDOT: PSS by the template stripping has demonstrated its beneficial effect on the device stability.

1. Introduction

The rapid development of organic light-emitting devices (OLEDs) in recent years makes them increasingly competitive in flat-panel display and solid-state lighting applications [1–9]. In particular, the flexibility of the OLEDs becomes a very attractive feature and has potential applications in flexible devices due to the sufficient ductibility of the organic materials. Indium tin oxide (ITO) is currently dominant transparent anode in OLEDs, due to its high optical transparency in most of the visible range, high electrical conductivity and high work function. However, ITO presents several key drawbacks, such as its high cost due to the scarcity of indium, its relatively high refractive index ($n_{ITO} \sim 2.0$), which induce power lost to the total internal reflection at the ITO/glass and ITO/organic interfaces [10] and its poor mechanical robust, which is unsuitable for applications in flexible devices [11]. There are several emerging materials that have shown promise for the replacement of ITO films, for example, metal grid [12], conducting polymer [12–17], carbon nanotube [18], graphene [19], and metal nanowire [20]. Among them, conducting polymer, particularly, poly(3,4-ethylene dioxythiophene): poly(styrene sulfonate) (PEDOT: PSS) has been attracted much attention for organic optoelectronic devices, because it enables cost-effective flexible devices as well as roll-to-roll mass production [21]. Several methods have been reported to enhance the conductivity of PEDOT: PSS [11–16]. The treatment method of dropping H_2SO_4 solutions on the dried PEDOT: PSS films had been employed to obtain high conductivity [15]. Unfortunately, the dropped H_2SO_4 will increase the surface roughness of the spin-coated PEDOT: PSS, and as well as results in a residue of the H_2SO_4 on the PEDOT: PSS surface, which is adverse to the device performance.

In this letter, we have demonstrated a flexible ITO-free OLED with ultrasmooth PEDOT: PSS anode by template

* Corresponding authors. Address: State Key Laboratory on Integrated Optoelectronics, College of Electronic Science and Engineering, Jilin University, 2699 Qianjin Street, Changchun 130012, People's Republic of China (H.-B. Sun). Tel./fax: +86 431 85168281.
E-mail addresses: jingfeng@jlu.edu.cn (J. Feng), hbsun@jlu.edu.cn (H.-B. Sun).

1566-1199/$ - see front matter © 2013 Elsevier B.V. All rights reserved.
http://dx.doi.org/10.1016/j.orgel.2013.11.035

stripping process [22–26] combined with the treatment method of dropping H_2SO_4. Compared to as-deposited PEDOT: PSS film on glass substrate, the template-stripped PEDOT: PSS film on polymer substrate has shown superiority on both conductivity and surface morphology. Its maximum current efficiency is 6.21 ± 0.43 cd/A, which corresponds to a 38% enhancement compared to that on the glass substrate. This improvement is obviously originated from hole-injection enhancement as a result of lowered surface roughness, and higher conductivity of PEDOT: PSS anode. The OLEDs based on the template-stripped PEDOT: PSS anodes on the polymer substrate have shown excellent flexibility, the devices are free of cracks and dark spots under a very small bending radius. In addition, the template stripping technique exhibits its effect on eliminating the H_2SO_4 residues on the anode surface, which is beneficial to the device stability.

2. Experimental details

2.1. Fabrication of PEDOT: PSS film on a flexible substrate

PEDOT: PSS aqueous solution (Clevios PH 1000) was purchased from Heraeus Clevios GmbH. The PEDOT: PSS films were prepared by spin coating the PEDOT: PSS aqueous solution on glass substrates at 2000 rpm for 30 s. The glass substrates were pre-cleaned with acetone, alcohol, and deionized water. The PEDOT: PSS films were dried at 120 °C on a hot plate for 15 min. The H_2SO_4 treatment was performed by dropping 100 μL H_2SO_4 (1 mol/L) solution on a PEDOT: PSS film on a hot plate at 160 °C. The films dried after about 5 min. They were cooled down to room temperature, and then were rinsed with deionized water. Finally, the polymer films were dried at 160 °C for about 5 min again. The thickness of PEDOT: PSS is decreased from 105.3 nm to 60.4 nm after the H_2SO_4 treatment. Then, a photopolymer (NOA63, Norland) film was spin coated onto the PEDOT: PSS film for 20 s at 1000 rpm and exposed to an ultraviolet light source for 5 min. The power of the light source is 125 W. At last, the cured photopolymer film can be peeled off as shown in Fig. 1(a). The photopolymer film has better adhesion with PEDOT: PSS than that with glass substrate, so that the PEDOT: PSS film can be peeled off with photopolymer and the flexible substrate with PEDOT: PSS was obtained. The thickness and refractive index of cured photopolymer substrate are around 400 μm and 1.56, respectively. Although the as-deposited PEDOT: PSS has a rough surface after H_2SO_4 treatment, the smoothness of the opposite interface is near that of the glass substrate. The surface morphology of peeled-off PEDOT: PSS will be almost identical with that of the glass surface. The surface morphology of both spin-coated PEDOT: PSS film on glass substrates and template-stripped PEDOT: PSS film on photopolymer substrates were measured by atomic force microscopy (AFM, iCON, Veeko). The sheet resistance and transmittance spectra of the PEDOT: PSS film were measured by a 4-point probe (ST-21H, 4probes Tech.) and a UV–Vis spectrophotometer (UV-2550, SHIMADZU Co., Inc., Japan), respectively.

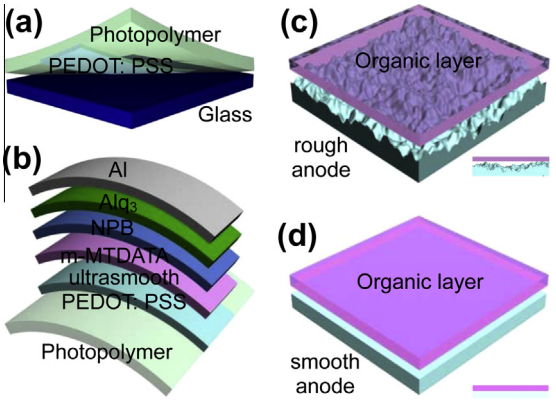

Fig. 1. Schematic of the template stripping process (a), structure of the flexible OLEDs (b), and the schematic for the contact area at the interface between the anode and the organic layer for the rough (c) and smooth (d) anode.

2.2. Fabrication and characterization of OLEDs

The OLEDs with the as-deposited PEDOT: PSS anode on glass substrates and ultrasmooth template-stripped PEDOT: PSS anode on photopolymer substrates were both fabricated. After the fabrication of the PEDOT: PSS anode, the glass and polymer substrate were put into thermal evaporation chamber. Then the organic layers and top contact were deposited layer by layer at a rate of 1 Å s^{-1} and at a base pressure of 5×10^{-4} Pa. 4,4′,4″-tris (3-methylphenylphe-nylamino) triphenylamine (m-MTDATA) and N,N′-diphenyl-N,N′-bis (1,1′-biphenyl)-4, 4′-diamine (NPB) were used as hole-injecting and transporting layers respectively. Tris-(8-hydroxyquinoline) aluminum (Alq_3) was used as emitting and electron-transporting layer. A 100-nm thick Al film was used as top cathode. LiF was inserted into the cathode and organic layers to enhance the electron injection. The detailed structure of OLED is PEDOT: PSS/m-MTDATA (30 nm)/NPB (20 nm)/Alq_3 (50 nm)/LiF (1 nm)/Al (100 nm) and shown in Fig. 1(b). A hole-only device with the structure of PEDOT: PSS/m-MTDATA (30 nm)/NPB (70 nm)/Al (100 nm) was also fabricated to investigate the effect of the ultrasmooth template-stripped PEDOT: PSS anode on the hole injection. Here, the active area of the device is 2×2 mm^2. The voltage–luminance and voltage–current density characteristics of the devices were measured by Keithley 2400 programmable voltage–current source and photo research PR-655 spectrophotometer. All of the measurements were conducted in air at room temperature.

3. Results and discussion

The surface morphology and conductivity of electrode plays a fundamental role in the behavior of OLEDs. The surface morphology of the bottom electrode will affect its contact area with the deposited organic layer as shown in Fig. 1(c) and (d). Generally, organic molecules are in form of large clusters when they deposited on an electrode by thermal evaporation, and they can not fill the depression of the rough electrode surface. Therefore, the contact

area between the electrode and the organic layer will decrease with the increased surface roughness of the bottom electrode. The contact area between PEDOT: PSS film and organic layer must be greatly increased with the increasing of the surface smoothness, so that the charge injection from PEDOT: PSS into the organic layer can be enhanced. The AFM images of the surface morphology for both as deposited and template-stripped PEDOT: PSS films have been shown in Fig. 2(a) and (b). Their root mean square (rms) roughness is 1.15 nm and 0.456 nm respectively, which demonstrates a much enhanced surface smoothness for the template-stripped PEDOT: PSS. The H_2SO_4-treated method has been employed to further enhance the conductivity of the PEDOT: PSS anode. The sheet resistance of the as-deposited PEDOT: PSS can be increased from over 20 000 Ω/□ for the untreated PEDOT: PSS to 70.36 Ω/□ for the H_2SO_4 treated PEDOT: PSS. For the as-deposited PEDOT: PSS, the surface morphology after the H_2SO_4 treatment were examined by AFM and shown in Fig. 2 (c). The rms roughness is 1.86 nm, which is higher than that before the H_2SO_4 treatment (1.15 nm). Therefore, the H_2SO_4-treated process will enlarge the rms roughness of the PEDOT: PSS surface. While, in case of the template-stripped PEDOT: PSS, the surface morphology of the opposite side for the peeled-off PEDOT: PSS would not be influenced by the H_2SO_4 treatment, so that the rms roughness of 0.468 nm (Fig. 2 (d)) is comparable to that of the untreated surface (0.456 nm). Besides the improved surface smoothness, the template-stripped PEDOT: PSS films also exhibit enhancement in the conductivity. Its sheet resistance is improved from 70.36 Ω/□ for the as-deposited PEDOT: PSS to 54.39 Ω/□. This enhancement is also originated from the improved surface morphology, because lower roughness is in favor of transport of carriers. Generally, charge transport in organic film is determined by scattering of conduction electrons at defects, grain boundaries, and surfaces. The charge transport within a single grain is easier and faster than that through the grain boundaries. In case of improved surface morphology, charge transport will be improved distinctly because of fewer grain boundaries for the films with smooth surface [27–30].

Fig. 3(a) presents the transmittance spectra in the visible range of PEDOT: PSS films without and with H_2SO_4 treatment on both glass and photopolymer substrate. The results indicate that the transmission of PEDOT: PSS before and after H_2SO_4 treatment are almost identical. Therefore, the H_2SO_4 treatment did not affect the transparency of the PEDOT: PSS film. Moreover, the transmittance of the PEDOT: PSS either on glass substrate or on photopolymer substrate is higher than 90% in the wavelength below 500 nm, and decreases a little but still higher than 80% at the wavelength above 500 nm. The current density–voltage characteristics of hole-only devices with the template-stripped and as-deposited PEDOT: PSS are compared and shown in Fig. 3(b). The current density of the hole-only devices with the template-stripped anode is obviously higher than that of the devices with the as-deposited anode. Both the improved conductivity induced by the improved surface smoothness and the increased carrier injection induced by the improved contact between the ultra-smooth electrode and organic film contribute to the enhanced current density.

The EL performance of the OLEDs with the ultrasmooth template-stripped and as-deposited PEDOT: PSS anode were investigated and summarized in Fig. 4. They exhibit identical EL spectra as can been seen in Fig. 4(a). Both current density and efficiency of the OLEDs with the ultra-smooth PEDOT: PSS anodes are obviously improved. Its maximum current efficiency is 6.21 ± 0.43 cd/A, while it is 4.71 ± 0.44 cd/A for that with the as-deposited PEDOT: PSS anode on glass substrate, which corresponds to 38% enhancement. These improvements arise from the enhancement in both conductivity and hole-injection as a result of the lowered surface roughness for the template-stripped PEDOT: PSS anode. Moreover, the efficiency of the template-stripped OLEDs is even higher than that of the devices based on ITO anode with the same device structure [31]. On the other hand, the template-stripped OLEDs based on the photopolymer substrates exhibit high flexibility. The photographs of the operating OLEDs before and after bending were shown in the inset of Fig. 4(b). There are no cracks and dark spots on OLEDs even at an almost completely folded bending.

There would remain H_2SO_4 residues after the H_2SO_4 treatment for the PEDOT: PSS surface, which may results in the damage to the organic molecules by the strong acid.

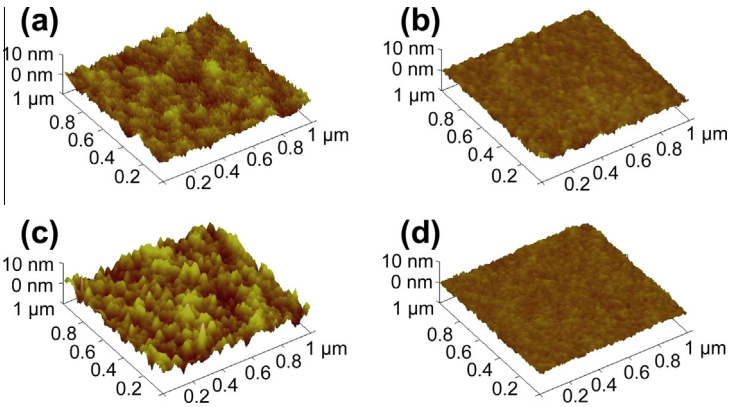

Fig. 2. Surface morphologies of the as-deposited (a) and template-stripped (b) PEDOT: PSS films without the H_2SO_4 treatment, and as-deposited (c) and template-stripped (d) PEDOT: PSS films with the H_2SO_4 treatment.

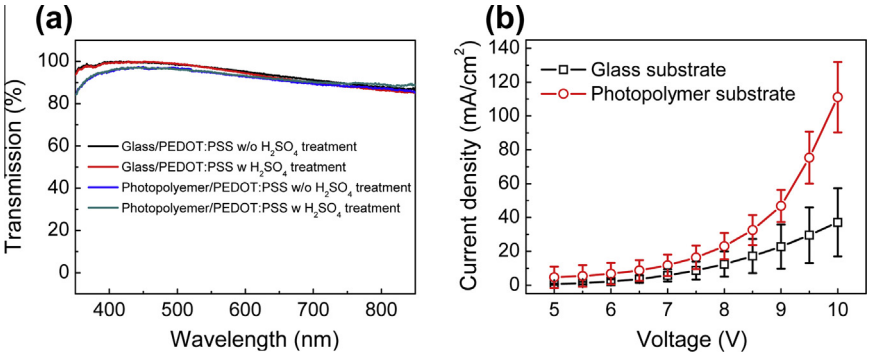

Fig. 3. (a) Transmittance spectra of PEDOT: PSS films of as-deposited and template-stripped without and with the H_2SO_4 treatment. (b) Current density–voltage characteristics of hole-only devices on glass and photopolymer substrate.

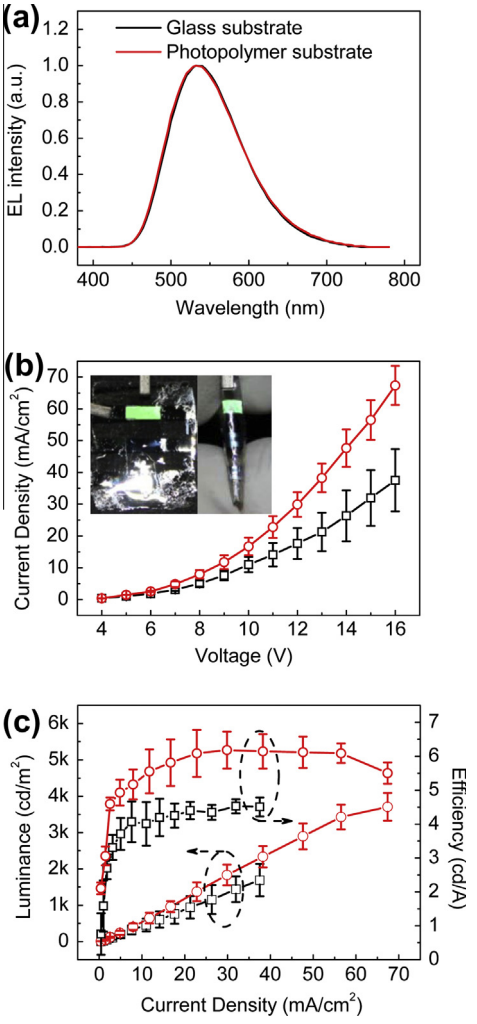

Fig. 4. EL performances of the OLEDs with the as-deposited anode on the glass substrate and template-stripped anode on the photopolymer substrate. (a) EL spectra, (b) current density–voltage and (c) luminance–current density–efficiency characteristics. The inset in (b) shows the photographs of the flexible OLEDs with the template-stripped anode on the photopolymer substrate before and after bending.

The organic molecules will contact with the opposite side of the PEDOT: PSS film in case of the template-stripped PEDOT: PSS, and the H_2SO_4 residues would be eliminated at this interface. The as-deposited and template-stripped PEDOT: PSS films before and after the H_2SO_4 treatment was characterized by X-ray photoelectron spectroscopy (XPS) to investigate the H_2SO_4 residues, and shown in Fig. 5(a)–(d). The two XPS peaks at 167.75 and 168.85 eV are the S_{2p} band of the sulfur atoms in PSS, whereas the two XPS peaks at 163.8 and 164.85 eV are that in PEDOT. In case of the H_2SO_4, the peak at 169.2 eV is the S_{2p} band of the sulfur atoms in the H_2SO_4 (Fig. 5(e)). The S_{2p} XPS intensity ratio of PEDOT to PSS saliently increases after the H_2SO_4 treatment, which indicates the removal of some PSSH chains from the PEDOT: PSS film. It is beneficial to the conductivity of PEDOT: PSS owing to the conduction of

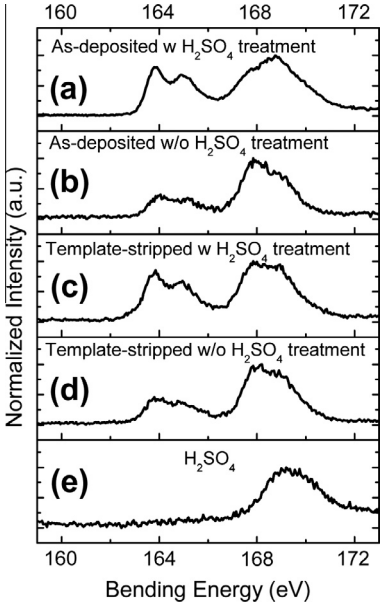

Fig. 5. XPS spectra of PEDOT: PSS and H_2SO_4 films. The as-deposited PEDOT: PSS films with (a) and without (b) H_2SO_4 treatment, template-stripped PEDOT: PSS films with (c) and without (d) H_2SO_4 treatment, and the H_2SO_4 (e).

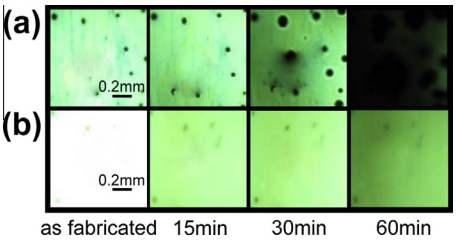

Fig. 6. Photographs of the operating flexible devices at different time with (a) and without (b) the H_2SO_4 residues.

PEDOT and the insulation of PSS. It can be seen in Fig. 5(a) that the peak at 168.85 eV was increased and higher than that at 167.75 eV, compared to that of the PEDOT: PSS film without the H_2SO_4 treatment (Fig. 5(b) and (d)). We can deduce that it may retain amount of H_2SO_4 after the H_2SO_4 treatment, because the peak at 168.85 eV is very close to that at 169.2 eV in the XPS spectra of H_2SO_4 (Fig. 5(e)). However, in case of the template-stripped PEDOT: PSS with the H_2SO_4 treatment (Fig. 5(c)), its XPS spectra is similar to that of the untreated films (Fig. 5(b) and (d)), which demonstrates that no H_2SO_4 residues on the opposite side of the PEDOT: PSS films. In addition, the XPS spectra indicate that the C/S molar ratio is 18.9% in as-deposited films and 18.3% in template-stripped films after the H_2SO_4 treatment, which indicates an identical removal of PSSH chains from the PEDOT: PSS film after the H_2SO_4 treatment. The above data demonstrates that the template stripping process can eliminate the residues of the H_2SO_4 on the PEDOT: PSS surface, and maintain its good conductivity.

To clarify the advantage of eliminating the H_2SO_4 residues on the device performance, the devices with residual H_2SO_4 have been fabricated as control. In this case, H_2SO_4 (0.5 mol/L) was doped into the PEDOT: PSS with ratio of 1:8, so that there remain the residues of the H_2SO_4 on the PEDOT: PSS surface after the template stripping. Photographs of the operating devices without encapsulation were shown in Fig. 6. The devices operate in highly humid atmosphere up to 75% RH at room temperature to accelerate its degradation. The driving voltage for the operating devices is 8 V. It is obvious that the devices with the residual H_2SO_4 exhibit more dark spots and both size and number of the dark spots increase quickly. The devices decay completely after 60 min operation. While in case of the devices without the residual H_2SO_4, less dark sports and more homogeneous luminance can be observed even after 60 min. Therefore the template stripping provides an avenue to persist the advantage of the conductivity improvement of the H_2SO_4 treatment on the PEDOT: PSS film, and avoid the disadvantage of the H_2SO_4 residues, which is very important for the application of this treatment.

4. Conclusions

In conclusion, an efficient ITO-free flexible OLED with ultrasmooth PEDOT: PSS anode has been demonstrated by template stripping process combined with the treatment method of dropping H_2SO_4. Compared to as deposited PEDOT: PSS film on glass substrate, the PEDOT: PSS film on polymer substrate fabricated by employing the template stripping process has shown superiority on both conductivity and surface morphology. The OLEDs based on the template-stripped PEDOT: PSS anode on the polymer substrate therefore exhibit improved efficiency and high flexibility. Moreover, the H_2SO_4 residues on the surface of the PEDOT: PSS induced from the H_2SO_4 treatment has been eliminated by the template stripping method, which demonstrates its beneficial effect on the OLED stability. From this research, we have confirmed that template stripping is an efficient and simple method to realize large area fabrication of conductive polymer, which are promising for cheaper flexible organic devices in manufacturing industries.

Acknowledgements

The authors gratefully acknowledge the financial support from the 973 Project (2013CBA01700 and 2011CB01300) and NSFC (Grant Nos. 61322402, 91233123, 61177024, and 61177090).

References

[1] S. Chen, L. Deng, J. Xie, L. Peng, L. Xie, Q. Fan, W. Huang, Recent developments in top-emitting organic light-emitting diodes, Adv. Mater. 22 (2010) 5227–5239.
[2] S. Reineke, F. Lindner, G. Schwartz, N. Seidler, K. Walzer, B. Lussem, K. Leo, White organic light-emitting diodes with fluorescent tube efficiency, Nature 459 (2009) 234–238.
[3] Y. Sun, N.C. Giebink, H. Kanno, B. Ma, M.E. Thompson, S.R. Forrest, Management of singlet and triplet excitons for efficient white organic light-emitting devices, Nature 440 (2006) 908–912.
[4] G. Lozano, D.J. Louwers, S.R.K. Rodriguez, S. Murai, O.T.A. Jansen, M.A. Verschuuren, J. Gomez Rivas, Plasmonics for solid-state lighting: enhanced excitation and directional emission of highly efficient light sources, Light Sci. Appl. 2 (2013) e66.
[5] C. Xiang, W. Koo, F. So, H. Sasabe, J. Kido, A systematic study on efficiency enhancements in phosphorescent green, red and blue microcavity organic light emitting devices, Light Sci. Appl. 2 (2013) e74.
[6] Q. Wang, Z. Deng, D. Ma, Realization of high efficiency microcavity top-emitting organic light-emitting diodes with highly saturated colors and negligible angular dependence, Appl. Phys. Lett. 94 (2009) 233303–233306.
[7] Y. Bai, J. Feng, Y.-F. Liu, J.-F. Song, J. Simonen, Y. Jin, Q.-D. Chen, J. Zi, H.-B. Sun, Outcoupling of trapped optical modes in organic light-emitting devices with one-step fabricated periodic corrugation by laser ablation, Org. Electron. 12 (2011) 1927–1935.
[8] P. Freitag, S. Reineke, S. Olthof, M. Furno, B. Lüssem, K. Leo, White top-emitting organic light-emitting diodes with forward directed emission and high color quality, Org. Electron. 11 (2010) 1676–1682.
[9] G. Xie, Z. Zhang, Q. Xue, S. Zhang, L. Zhao, Y. Luo, P. Chen, B. Quan, Y. Zhao, S. Liu, Highly efficient top-emitting white organic light-emitting diodes with improved contrast and reduced angular dependence for active matrix displays, Org. Electron. 11 (2010) 2055–2059.
[10] K. Saxena, V.K. Jain, D.S. Mehta, A review on the light extraction techniques in organic electroluminescent devices, Opt. Mater. 32 (2009) 221–233.
[11] M. Cai, Z. Ye, T. Xiao, R. Liu, Y. Chen, R.W. Mayer, R. Biswas, K.-M. Ho, R. Shinar, J. Shinar, Extremely efficient indium-tin-oxide-free green phosphorescent organic light-emitting diodes, Adv. Mater. 24 (2012) 4337–4342.
[12] M.-G. Kang, M.-S. Kim, J. Kim, L.J. Guo, Organic solar cells using nanoimprinted transparent metal electrodes, Adv. Mater. 20 (2008) 4408–4413.
[13] Y.H. Kim, C. Sachse, M.L. Machala, C. May, L. Müller-Meskamp, K. Leo, Highly conductive PEDOT: PSS electrode with optimized solvent and thermal post-treatment for ITO-free organic solar cells, Adv. Funct. Mater. 21 (2011) 1076–1081.

[14] M. Vosgueritchian, D.J. Lipomi, Z. Bao, Highly conductive and transparent PEDOT: PSS films with a fluorosurfactant for stretchable and flexible transparent electrodes, Adv. Funct. Mater. 22 (2012) 421–428.
[15] Y. Xia, K. Sun, J. Ouyang, Solution-processed metallic conducting polymer films as transparent electrode of optoelectronic devices, Adv. Mater. 24 (2012) 2436–2440.
[16] K. Fehse, K. Walzer, K. Leo, W. Lövenich, A. Elschner, Highly conductive polymer anodes as replacements for inorganic materials in high-efficiency organic light-emitting diodes, Adv. Mater. 19 (2007) 441–444.
[17] M. Cai, T. Xiao, R. Liu, Y. Chen, R. Shinar, J. Shinar, Indium-tin-oxide-free tris(8-hydroxyquinoline) Al organic light-emitting diodes with 80% enhanced power efficiency, Appl. Phys. Lett. 99 (2011) 153303.
[18] M.W. Rowell, M.A. Topinka, M.D. McGehee, H.-J. Prall, G. Dennler, N.S. Sariciftci, L. Hu, G. Gruner, Organic solar cells with carbon nanotube network electrodes, Appl. Phys. Lett. 88 (2006) 233506.
[19] L. Gomez De Arco, Y. Zhang, C.W. Schlenker, K. Ryu, M.E. Thompson, C. Zhou, Continuous, highly flexible, and transparent graphene films by chemical vapor deposition for organic photovoltaics, ACS Nano 4 (2010) 2865–2873.
[20] J. Meiss, M.K. Riede, K. Leo, Towards efficient tin-doped indium oxide (ITO)-free inverted organic solar cells using metal cathodes, Appl. Phys. Lett. 94 (2009) 013303.
[21] F.C. Krebs, S.A. Gevorgyan, J. Alstrup, A roll-to-roll process to flexible polymer solar cells: model studies, manufacture and operational stability studies, J. Mater. Chem. 19 (2009) 5442–5451.
[22] N.C. Lindquist, T.W. Johnson, D.J. Norris, S.-H. Oh, Monolithic integration of continuously tunable plasmonic nanostructures, Nano Lett. 11 (2011) 3526–3530.
[23] P. Nagpal, N.C. Lindquist, S.-H. Oh, D.J. Norris, Ultrasmooth patterned metals for plasmonics and metamaterials, Science 325 (2009) 594–597.
[24] M. Hegner, P. Wagner, G. Semenza, Ultralarge atomically flat template-stripped Au surfaces for scanning probe microscopy, Surf. Sci. 291 (1993) 39–46.
[25] Y.-F. Liu, J. Feng, H.-F. Cui, D. Yin, J.-F. Song, Q.-D. Chen, H.-B. Sun, Highly flexible inverted organic solar cells with improved performance by using an ultrasmooth Ag cathode, Appl. Phys. Lett. 101 (2012) 133303.
[26] Y.F. Liu, J. Feng, D. Yin, Y.G. Bi, J.F. Song, Q.D. Chen, H.B. Sun, Highly flexible and efficient top-emitting organic light-emitting devices with ultrasmooth Ag anode, Opt. Lett. 37 (2012) 1796–1798.
[27] J.-F. Salinas, H.-L. Yip, C.-C. Chueh, C.-Z. Li, J.-L. Maldonado, A.K.Y. Jen, Optical design of transparent thin metal electrodes to enhance in-coupling and trapping of light in flexible polymer solar cells, Adv. Mater. 24 (2012) 6362–6367.
[28] S. Verlaak, V. Arkhipov, P. Heremans, Modeling of transport in polycrystalline organic semiconductor films, Appl. Phys. Lett. 82 (2003) 745–747.
[29] S. Steudel, S. De Vusser, S. De Jonge, D. Janssen, S. Verlaak, J. Genoe, P. Heremans, Influence of the dielectric roughness on the performance of pentacene transistors, Appl. Phys. Lett. 85 (2004) 4400–4402.
[30] Y.-F. Liu, J. Feng, H.-F. Cui, Y.-F. Zhang, D. Yin, Y.-G. Bi, J.-F. Song, Q.-D. Chen, H.-B. Sun, Fabrication and characterization of Ag film with sub-nanometer surface roughness as a flexible cathode for inverted top-emitting organic light-emitting devices, Nanoscale 5 (2013) 10811–10815.
[31] D.D. Zhang, J. Feng, H. Wang, Y.-F. Liu, L. Chen, Y. Jin, Y.-Q. Zhong, Y. Bai, Q.-D. Chen, H.-B. Sun, Efficiency enhancement in organic light-emitting devices with a magnetic doped hole-transport layer, Photonics J. IEEE 3 (2011) 26–30.